ISSN 1063-7761, Journal of Experimental and Theoretical Physics, 2010, Vol. 111, No. 1, pp. 135–145. © Pleiades Publishing, Inc., 2010.
Original Russian Text © I.A. Budagovsky, A.S. Zolot'ko, M.P. Smayev, M.I. Barnik, 2010, published in Zhurnal Éksperimental'noĭ i Teoreticheskoĭ Fiziki, 2010, Vol. 138, No. 1, pp. 150–161.

STATISTICAL, NONLINEAR, AND SOFT MATTER PHYSICS

Self-Action of a Light Beam in Nematic Liquid Crystals in the Presence of a DC Electric Field

I. A. Budagovsky[a], A. S. Zolot'ko[a], M. P. Smayev[a], and M. I. Barnik[b]

[a] *Lebedev Physical Institute, Russian Academy of Sciences, Leninskii pr. 53, Moscow, 119991 Russia*

[b] *Shubnikov Institute of Crystallography, Russian Academy of Sciences, Leninskii pr. 59, Moscow, 119333 Russia*

e-mail: zolotko@sci.lebedev.ru

Received November 24, 2009

Abstract—The results of experimental study of the light beam self-action in a nematic liquid crystal placed in a dc electric field are presented, and a theory of this effect is developed. This self-action of a light beam is shown to cause a hyperbolic umbilic caustic. The intensity distribution and caustics calculated in the far diffraction zone of the light beam agree well with the experimental data.

DOI: 10.1134/S1063776110070137

1. INTRODUCTION

Applied fields can easily change the orientational structure (director field) of nematic liquid crystals (NLCs) [1, 2]. The reorientation of a director in an NLC in a low-frequency electric field serves as the basis for the application of NLCs in data displays. The rotation of a director by a light field leads to a giant orientational optical nonlinearity, which is nine orders of magnitude higher than the Kerr nonlinearity of usual liquids [3]. The orientational nonlinearity induced by absorbing additions is higher by other two orders of magnitude [4, 5]. When a light beam interacts with an NLC, an effective self-action (self-focusing [3, 6–14] or self-defocusing [5, 14, 15]) is observed. If a Gaussian light beam passes through an oriented NLC layer about 100 μm thick, the intensity distribution in its cross section in the far diffraction zone changes qualitatively. This distribution (aberration pattern) has the shape of concentric rings [6–8, 11, 14] and corresponds to a domelike transverse profile of the refractive index. A ring aberration pattern is also characteristic of self-action in liquids [16, 17] and other media.

An aberration pattern gives rather comprehensive information on the interaction of light with NLC. It can be used to determine the sign of self-action [14], the angle of director rotation in the NLC volume and its dynamics [7, 18–20], the ratio of elastic constants [9], and the angle of director orientation at the NLC walls using the effect of nonlinear rotation of a polarization plane [21].

An ac electric field suppresses or strengthens the optical nonlinearity [22, 23] and can result in various types of optical bistability [24–27]. In this case, the ring shape of an aberration pattern remains unchanged.

If a dc electric field affects an NLC, the self-action of light becomes qualitatively different [28, 29]. The aberration pattern in the far diffraction zone becomes strongly asymmetric, the ring structure disappears, and a kink is observed at the pattern boundary. A dc voltage of 2 V applied to an NLC increases the nonlinearity by two orders of magnitude, i.e., identically to the increase induced by light-absorbing additions.

The purpose of this work is to present the main experimental results of the study of the light beam interaction with an NLC in a dc electric field and to develop a theory for this phenomenon.

2. EXPERIMENTAL RESULTS

The radiation of a continuous argon ($\lambda = 515$ nm) or solid-state ($\lambda = 473$ nm) laser (lowest Gaussian mode) was focused by a lens with a focal distance of 16 cm (the beam waist diameter was about 100 μm) on a planar 100-μm-thick sample of a ZhKM-1277 nematic matrix [5]. A dc voltage was applied to the sample via semiconductor (indium and tin oxide) electrodes deposited onto glass substrates. The planar orientation was achieved by rubbing of polyimide layers deposited onto the electrodes by centrifugation and polymerized at a high temperature.

A liquid-crystal cell could rotate through angle α about the vertical axis (angle α was taken to be positive for clockwise NLC rotation), and the NLC director was placed in the horizontal plane. Angle φ made by the direction of linear light-beam polarization with the plane of incidence (horizontal plane) could change from 0° (extraordinary wave) to 90° (ordinary wave). The polarity of the applied dc voltage was conventionally considered to be positive when the entrance (with respect to the beam) substrate represented an anode.

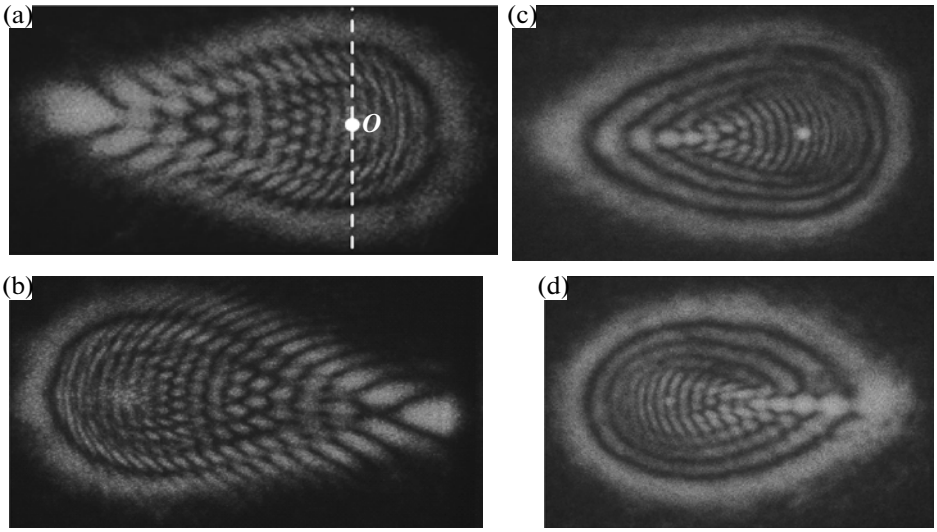

Fig. 1. Aberration patterns for an obliquely incident light beam ($\lambda = 515$ nm) having passed through a planar NLC: (a, b) ZhKM-1277, $P = 20$ mW, $\alpha = -40°$, extraordinary wave, and applied dc voltage $U =$ (a) +3 and (b) −3 V; (c, d) ZhKM-1277 + 0.1% methyl red, $P = 5$ mW, ordinary wave, $U = +2$ V, and $\alpha =$ (c) −60° and (d) +60°.

Figure 1a shows the stationary aberration pattern that appears when an obliquely incident ($\alpha = -40°$) light beam with extraordinary polarization passes through the planar NLC. The time it takes for the pattern to form is several tens of seconds, which corresponds to the characteristic director reorientation time. This pattern is asymmetric with respect to the vertical: it is elongated to the left, and the pattern boundary has a kink (in the form of an acute angle) on this side.

A change in the sign of angle of light incidence α or the polarity of dc voltage U (Fig. 1b) "reflects" the aberration pattern with respect to the vertical line (Fig. 1a, dashed line) that passes through point O (which is the center of the light beam before the development of self-action).

The aberration pattern in the NLC in the presence of a dc electric field (as compared to the ring pattern) is characterized by its dependence on the light polarization. The rotation of the polarization plane from the horizontal decreases the pattern intensity but does not change the intensity distribution (except for the central point, where a bright spot appears). The polarization of the pattern remains horizontal (extraordinary wave), and the polarization of the spot at the center is vertical (ordinary wave).

The character of the dependence of the aberration pattern on the light polarization means that the polarization does not affect the deformation of the director field. Since the direct effect of the light field depends substantially on the polarization (e.g., for planar samples, the light-induced reorientation under the action of an ordinary wave is almost absent [30]), the director reorientation in our case should be related to the surface photorefractive effect, i.e., to the action of a dc field. The role of light consists in the removal of the screening of the applied electric field by surface charges, which can be localized at the NLC–polyimide and polyimide–electrode interfaces. The screening of a dc electric field is experimentally supported by a fourfold difference in the Fréedericksz transition thresholds in ac (0.95 V at 3 kHz) and dc (3.8 V) fields.

Qualitative differences between the asymmetric and ring patterns are also observed in the transformation of the intensity distribution during a rapid (shorter than 1 s) shift of the NLC with respect to the light beam. In this case, the director field has no time to transform, and the light beam is actually probing. In the case of the standard ring aberration pattern of self-defocusing, the bottom part of the pattern becomes brighter when the NLC shifts up and the intensity of the top part decreases. Upon self-focusing, the top part of the pattern becomes brighter and the intensity of the bottom part decreases [14]. When the NLC shifts in any other direction, the transformation of the pattern can easily be traced by analyzing the axial symmetry of the director field. In the case of our asymmetric aberration pattern, when the NLC shifts upward, the lower pattern boundary becomes brighter and the intensity of the upper boundary decreases (Fig. 2b). In this case, however, a certain region in the top part of the pattern also becomes brighter (Fig. 2b, dashed line). When the crystal shifts to the left (Fig. 2d), the central portion of the pattern becomes brighter (the initial boundary is almost invisible); when the crystal shifts to the right, the intensity of the central portion decreases slightly. This complex character of intensity transformation indicates a qualitative difference between the phase front and the director field forming it, on the one hand, and corresponding characteristics in the case of the conventional self-action, on the other.

We now develop a quantitative model for the self-action of light in an NLC in the presence of a dc field.

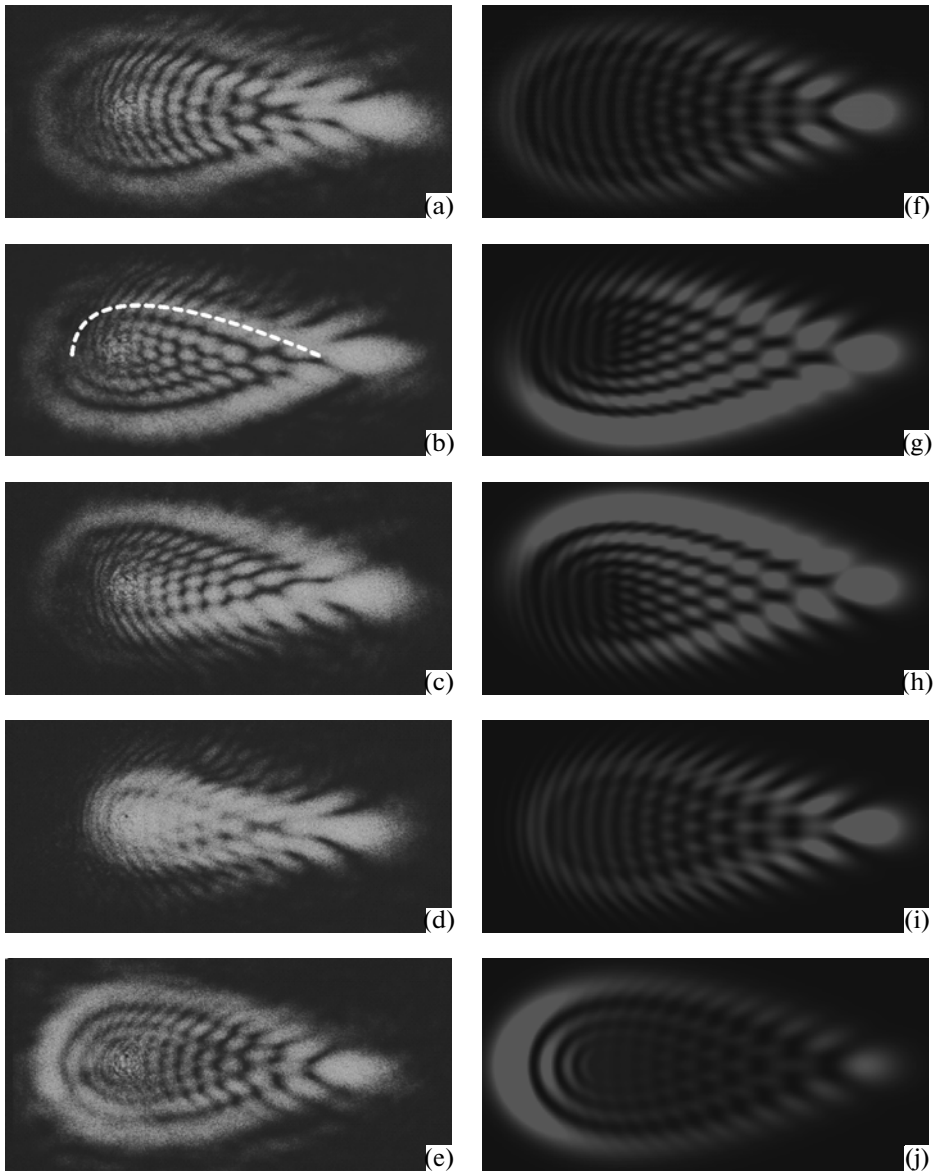

Fig. 2. (a–e) Aberration patterns detected in the far diffraction zone when a cell with a ZhKM-1277 NLC is illuminated by an obliquely incident ($\alpha = +40°$) laser beam ($\lambda = 515$ nm, $P = 10$ mW) at an applied dc voltage $U = +2$ V. (f–j) Results of numerical calculation at a beam waist $w_0 = 70$ μm, $\Delta n = 0.2$, $\gamma_A^2 = 0.6$, $\gamma_C = 0$, $\eta = 0$, $\beta = +30°$, and $l_A = 150$ μm. The crystal shifts (b, g) up, (c, h) down, (d, i) to the left and (e, j) to the right with respect to the beam. The patterns in (g–j) were calculated at a crystal shift of $0.5w_0$ with respect to the beam. The horizontal and vertical sizes of all patterns are 0.1 and 0.05 rad, respectively.

3. CALCULATION OF THE ABERRATION PATTERN OF THE SELF-ACTION OF A LIGHT BEAM AND COMPARISON WITH EXPERIMENTAL DATA

When passing through the layer of a liquid crystal, a light beam with extraordinary polarization (propagating along the y axis in Fig. 3) acquires additional phase shift $S_{NL}(x, z)$ related to the nonlinearity of the NLC—the change induced in the refractive index during the director rotation caused by the light field. The initially plane front acquires the form

$$y = -S_{NL}(x, z)/k + \text{const}, \quad k = 2\pi/\lambda.$$

Angles θ_x and θ_z of deflections of the horizontal and vertical rays, which are characterized by coordinates x and z, are

$$\theta_x = \frac{1}{k}\frac{\partial S_{NL}}{\partial x}, \quad \theta_z = \frac{1}{k}\frac{\partial S_{NL}}{\partial z}. \tag{1}$$

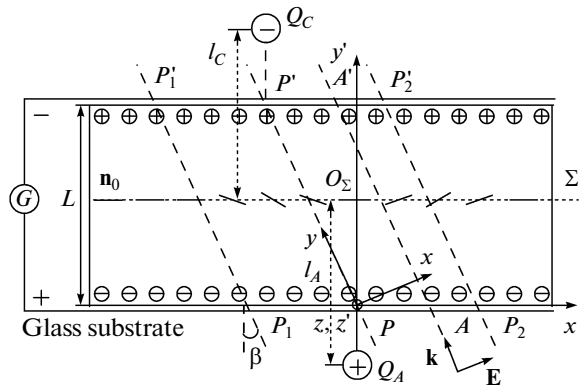

Fig. 3. Light-induced reorientation of the director in an NLC in the presence of a direct current electric field: PP' is the axial ray of the light beam; P_1P_1' and P_2P_2', peripheral rays (conventional boundary of the light beam); AA', arbitrary ray of the light beam; Q_A and Q_C, point charges simulating the light field–induced removal of screening; bars in plane Σ equidistant from the NLC boundaries indicate the director orientation (for the case $Q_C = 0$); l_A and l_C, distances from the charges to plane Σ; L, the liquid-crystal layer thickness; $\mathbf{k}$ and $\mathbf{E}$, wavevector and electric field of a light wave, respectively; and β, angle of refraction (change in the direction of ray propagation at the glass substrate–NLC interface is not shown).

The intensity distribution in the aberration pattern is calculated by the Kirchhoff formula

$$I(\theta_x, \theta_z) = \frac{k^2}{4\pi^2 y^2}\left|\int_{-\infty-\infty}^{\infty\ \infty} I_0(x, z) \times \exp[-ik(\theta_x x + \theta_z z) + iS_{NL}(x, z)]dxdz\right|^2, \quad (2)$$

where $I_0(x, z)$ is the intensity distribution in the xz plane. Equations (1) determine the mapping of the xz plane onto the $\theta_x\theta_z$ plane. The critical points of this mapping, i.e., the points at which the Jacobian of the transformation vanishes,

$$\frac{D(\theta_x, \theta_z)}{D(x, z)} = 0, \quad (3)$$

correspond to caustics in the far diffraction zone. According to the theory of the singularities of smooth mapping [31–36], which is also called the theory of catastrophes, function $S_{NL}(x, z)$ in the vicinity of the critical points can be reduced to one of the normal forms, each of which corresponds to a certain type of singularity ("elementary catastrophe").

We have to calculate the nonlinear phase shift in the cross section of the light beam in order to determine the light beam intensity distribution in the far diffraction zone, to find caustics, and to reveal the character of their singularities. The determination of the deformed director field is a necessary stage of this calculation.

3.1. Light-Induced Reorientation of the NLC Director in a DC Electric Field

To calculate the deformed director field $\mathbf{n}(\mathbf{r})$, we use the one-constant approximation; i.e., all three Franck elastic constants are taken to be equal. This widely used approximation qualitatively correctly describes the director field [1, 2, 37]. Density F of the free energy of the NLC in electric field $\mathbf{G}$ is

$$F = \frac{K}{2}(\mathrm{div}^2\mathbf{n} + \mathrm{curl}^2\mathbf{n}) - \frac{\Delta\varepsilon_{dc}(\mathbf{n}\cdot\mathbf{G})^2}{8\pi}, \quad (4)$$

where K is the Franck elastic constant and $\Delta\varepsilon_{dc}$ is the anisotropy of the permittivity in a dc field. When writing the free-energy density in the form of (4), we neglect the term describing the interaction of the NLC with the light field. As a result, we do not take into account the direct orientational action of light on the NLC. We vary Eq. (4) with allowance for the condition $\mathbf{n}^2 = 1$ and obtain

$$\Delta\mathbf{n} + \frac{\Delta\varepsilon_{dc}(\mathbf{n}\cdot\mathbf{G})\mathbf{G}}{4\pi K} = -\frac{\lambda(\mathbf{r})}{K}\mathbf{n}, \quad (5)$$

where $\lambda(\mathbf{r})$ is the Lagrange multiplier. This multiplier can be excluded using the vector multiplication of Eq. (5) by $\mathbf{n}$,

$$\Delta\mathbf{n}\times\mathbf{n} + \frac{\Delta\varepsilon_{dc}}{4\pi K}(\mathbf{G}\cdot\mathbf{n})\mathbf{G}\times\mathbf{n} = 0. \quad (6)$$

We search for the deformed director field using a perturbation theory and assuming $\mathbf{n} = \mathbf{n}_0 + \delta\mathbf{n}$, where $\mathbf{n}_0$ is the unperturbed director and $\delta\mathbf{n}$ is the desired vector function satisfying the condition $\mathbf{n}_0\cdot\delta\mathbf{n} = 0$. Using Eq. (6), we obtain the following linear equation for $\delta\mathbf{n}$:

$$\Delta\delta\mathbf{n} + \frac{\Delta\varepsilon_{dc}}{4\pi K}(\mathbf{G}\cdot\mathbf{n}_0)[\mathbf{n}_0\times\mathbf{G}]\times\mathbf{n}_0 = 0. \quad (7)$$

Equation (7) can be analytically solved only after certain simplifications. We introduce the following Cartesian coordinates: the x' axis lies in the horizontal plane and is parallel to the NLC walls, the y' axis is normal to the walls, and the z' axis is vertical (Fig. 3). We first neglect the second derivatives with respect to transverse coordinates x' and z' in Eq. (7). In this case, the elastic forces that tend to smooth the transverse nonuniformity of the director field are excluded. As a result, the director orientation in the line connecting points $(x', 0, z')$ and (x', L, z') depends only on the electric field in this line. Strictly speaking, this simplification is valid if the light beam width is much larger than the NLC thickness. Nevertheless, after the transverse elastic forces are neglected, the solution to Eq. (7) can adequately reflect the character of the transverse dependence of the director field (which is determined by the transverse profile of the electric field). We then perform longitudinal smoothing of the electric field. The electric field is assumed to be independent of transverse coordinate y; let it be equal to

the value at $y' = L/2$ (i.e., at points in plane Σ that is equidistant from the NLC boundaries), $G(x', y', z') = G(x', L/2, z') = G_c(x', z')$. As a result, we arrive at the ordinary differential equation

$$\frac{d^2\delta\mathbf{n}}{d^2y'} + \frac{\Delta\varepsilon_{dc}}{4\pi K}(\mathbf{G}_c \cdot \mathbf{n}_0)[\mathbf{n}_0 \times \mathbf{G}_c] \times \mathbf{n}_0 = 0. \quad (8)$$

The solution to Eq. (8) is sought using the Galerkin method on the assumption

$$\delta\mathbf{n}(x', y', z') = \delta\mathbf{n}_m(x', z')\sin\pi y'/L \quad (9)$$

(coordinates x' and z' are now parameters). Equation (9) corresponds to rigid boundary conditions (the surface forces are high and specify the direction at the crystal boundary that is independent of the deformed director field [38]) and coincides with the exact solution to the problem of the direction reorientation in a homogeneous field at low angles of director rotation. We substitute solution (9) into Eq. (8), multiply the obtained expression by $\sin(\pi y'/L)$, average it over the NLC volume, and find the following expression for the deformation of the director field in an inhomogeneous field:

$$\delta\mathbf{n}_m = \frac{\Delta\varepsilon_{dc}L^2}{\pi^4 K}(\mathbf{G}_c \cdot \mathbf{n}_0)[\mathbf{n}_0 \times \mathbf{G}_c] \times \mathbf{n}_0. \quad (10)$$

The electric field applied to the NLC is screened by surface charges (see Fig. 3). The action of light partly removes this screening. This effect is simulated by the field of two point charges (positive (Q_A) and negative (Q_C) charges) located at distances l_A and l_C from plane Σ (subscripts A and C correspond to the anode and cathode, respectively). The charges are situated in the lines normal to the crystal substrates and passing through the points of entrance of the axial ray of the light beam into the NLC and exit from it (which corresponds to the maximum degree of screening removal on the beam axis). The corresponding expression for the electric field inside the liquid-crystal layer is

$$\mathbf{G}_c = \frac{Q_A(\mathbf{i}x' + \mathbf{j}l_A + \mathbf{k}z')}{\varepsilon_{dc}(x'^2 + l_A^2 + z'^2)^{3/2}} + \frac{Q_C[\mathbf{i}(x' + L\tan\beta) + \mathbf{j}l_C + \mathbf{k}z']}{\varepsilon_{dc}[(x' + L\tan\beta)^2 + l_C^2 + z'^2]^{3/2}} + \mathbf{j}\eta G_0, \quad (11)$$

where $\mathbf{i}, \mathbf{j}, \mathbf{k}$ are the unit vectors along the x', y', z' axes; $G_0 = U/L$; β is the angle of refraction of the light beam at the glass substrate–NLC interface, which is related to angle of incidence α by the simple relationship $\sin\alpha/\sin\beta = n_e$ (where n_e is the refractive index of the extraordinary wave in the NLC); and η is the parameter characterizing the degree of screening of the applied field by surface charges in the absence of light radiation ($\eta = 0$ corresponds to complete screening). We substitute Eq. (11) into Eq. (10) and finally obtain

$$\delta\mathbf{n}_m = \frac{4}{\pi}\left\{\gamma_A\frac{l_A^2 x'}{(x'^2 + l_A^2 + z'^2)^{3/2}} + \gamma_C\frac{l_C^2(x' + L\tan\beta)}{[(x' + L\tan\beta)^2 + l_C^2 + z'^2]^{3/2}}\right\} \times \left\{\gamma_A\frac{l_A^2(\mathbf{j}l_A + \mathbf{k}z')}{(x'^2 + l_A^2 + z'^2)^{3/2}} + \gamma_C\frac{l_C^2(\mathbf{j}l_C + \mathbf{k}z')}{[(x' + L\tan\beta)^2 + l_C^2 + z'^2]^{3/2}} + \mathbf{j}\gamma_G\right\}, \quad (12)$$

where

$$\gamma_A = \frac{Q_A}{Q_{A,\,\mathrm{th}}}, \quad \gamma_C = \frac{Q_C}{Q_{C,\,\mathrm{th}}},$$

$$\gamma_G = \frac{\eta G_0}{G_{\mathrm{th}}}, \quad G_{\mathrm{th}} = \frac{\pi}{L}\sqrt{\frac{4\pi K}{\Delta\varepsilon_{dc}}},$$

G_{th} is the Fréedericksz transition threshold in a dc field,

$$G_{A,\,\mathrm{th}} = l_A^2\varepsilon_{dc}G_{\mathrm{th}}, \quad Q_{C,\,\mathrm{th}} = l_C^2\varepsilon_{dc}G_{\mathrm{th}}.$$

3.2. Nonlinear Phase Shift for the Light Beam

The refractive index of an extraordinary wave in a uniaxial anisotropic medium is

$$n_e = \frac{\sqrt{\varepsilon_\perp\varepsilon_\parallel}}{\sqrt{\varepsilon_\perp + \Delta\varepsilon(\boldsymbol{\kappa}\cdot\mathbf{m})^2}}, \quad (13)$$

where $\varepsilon_\parallel$ and $\varepsilon_\perp$ are the principal values of the permittivity tensor at the light frequency, $\Delta\varepsilon = \varepsilon_\parallel - \varepsilon_\perp$, $\boldsymbol{\kappa} = \mathbf{k}/k$, $\mathbf{k}$ is the wavevector of the light beam, and $\mathbf{m}$ is the unit vector directed along the optical axis. We take into account the smallness of the parameter $\delta n_e = \varepsilon_\parallel^{1/2}\Delta\varepsilon/2\varepsilon_\perp$, use the relationship $\mathbf{m} = (\mathbf{n}_0 + \delta\mathbf{n})/|\mathbf{n}_0 + \delta\mathbf{n}|$, and represent the refractive index corresponding to the deformed director field as the following expansion in powers of $\delta\mathbf{n}$:

$$n_e = n_e^{(0)} + n_e^{(1)} + n_e^{(2)}, \quad (14)$$

where

$$n_e^{(0)} = \sqrt{\varepsilon_\parallel} - \delta n_e(\boldsymbol{\kappa}\cdot\mathbf{n}_0)^2,$$

$$n_e^{(1)} = -2\delta n_e(\boldsymbol{\kappa}\cdot\mathbf{n}_0)(\boldsymbol{\kappa}\cdot\delta\mathbf{n}),$$

$$n_e^{(2)} = \delta n_e[(\boldsymbol{\kappa}\cdot\mathbf{n}_0)^2\delta\mathbf{n}^2 - (\boldsymbol{\kappa}\cdot\delta\mathbf{n})^2].$$

Nonlinear phase shift $S_{NL}(x', z')$ for arbitrary ray AA' that enters into the liquid-crystal layer at point A with

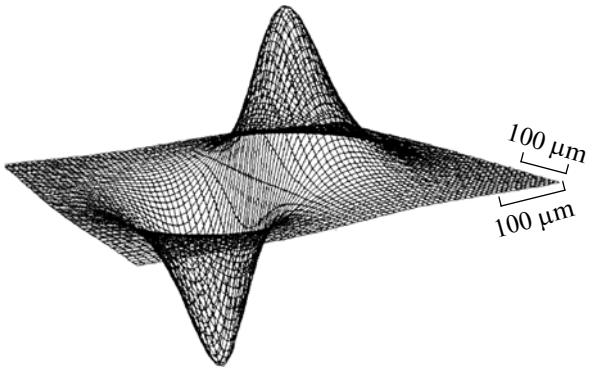

Fig. 4. Phase shift (16) of the light beam having passed through an NLC ($L = 100$ μm, $\gamma_A^2 = 0.6$, $\gamma_C = 0$, $\eta = 0$, $\Delta n = 0.2$, $\beta = +30°$, $\lambda = 515$ nm). The amplitudes of the left and right "bells" are −36 and +30, respectively.

coordinates $(x', 0, z')$ and exits from it at point A' $(x_1' = x' - L\tan\beta, L, z')$ (see Fig. 3) is represented as the integral

$$S_{NL} = \frac{2\pi}{\lambda} \times \int_A^{A'} [n_e^{(1)}(x', y', z') + n_e^{(2)}(x', y', z')]ds'. \quad (15)$$

We expand the integrand in coordinate x with respect to point $(x' + x_1')/2$, restrict ourselves to constant and linear terms, and find

$$S_{NL} = S_{NL}^{(1)} + S_{NL}^{(2)}, \quad (16)$$

where

$$S_{NL}^{(1)} = 2S_0 gh\sin\beta, \quad (17)$$

$$S_{NL}^{(2)} = \frac{S_0 g^2}{\cos\beta}(-h^2\cos 2\beta + r^2\sin^2\beta) \quad (18)$$

are the contributions to the nonlinear phase shift that are proportional to the first and second powers of director field deformation $\delta\mathbf{n}$. Here,

$$g = \frac{\gamma_A u}{(1 + u^2 + v^2)^{3/2}} + \frac{\gamma_C(pu + s)}{[1 + (pu + s)^2 + p^2 v^2]^{3/2}}; \quad (19)$$

$$h = \frac{\gamma_A}{(1 + u^2 + v^2)^{3/2}} - \frac{\gamma_C}{[1 + (pu + s)^2 + p^2 v^2]^{3/2}} + \gamma_G; \quad (20)$$

$$r = \frac{\gamma_A v}{(1 + u^2 + v^2)^{3/2}} - \frac{\gamma_C v}{[1 + (pu + s)^2 + p^2 v^2]^{3/2}}; \quad (21)$$

and

$$S_0 = 16\delta n_e L/\pi\lambda, \quad p = l_A/l_C, \quad s = L\tan\beta/l_C,$$

$$u = (x' - L\tan\beta/2)/l_A, \quad v = z'/l_A$$

are dimensionless coordinates.

3.3. Numerical Calculation of the Aberration Pattern and Caustics

Figure 2f shows the aberration pattern for a Gaussian light beam $I_0(x, z) \propto \exp[-(x^2 + z^2)/w_0^2]$ with beam waist w_0 that was calculated by Eqs. (2) and (16) with allowance for the relation $x = x'/\cos\beta$ for parameters $\gamma_A^2 = 0.6$, $\gamma_C = 0$, $\eta = 0$, $\Delta n = 0.2$, and $\beta = +30°$. Figure 4 shows corresponding phase shift (16), which includes linear (Eq. (17)) and quadratic (Eq. (18)) contributions.

The calculated aberration pattern agrees well with the experimental pattern (see Fig. 2a). Parameter γ_A served as an adjustable parameter for the calculation. In our model, this parameter determines the maximum angle of director rotation. Parameter l_A was taken to be 150 μm (i.e., the distance from charge Q_A to the liquid-crystal layer was equal to layer thickness L). Parameter l_A controls the transverse size of director deformation and affects the angular spread of the beam. As follows from Fig. 4, the phase shift can be considered in a certain approximation as a sum of two bell-shaped surfaces of different signs. The concave "bell" corresponds to a decrease in the refractive index (i.e., self-defocusing of the corresponding part of the beam), and the convex bell corresponds to an increase in the refractive index (self-focusing). This shape of phase shift can easily be understood from Fig. 3. Indeed, for the rays intersecting plane Σ on the right of point O_Σ (e.g., for ray AA'), the director rotates to be parallel to light field $\mathbf{E}$, increasing the refractive index of the extraordinary wave. For the rays passing on the left of point O_Σ, the converse situation takes place and the refractive index decreases.

Figures 5a1 and 5a2 show the sets of critical points obtained by numerical solution of Eq. (3) and the corresponding caustics calculated by Eqs. (1). For the calculations, we used the parameters from Fig. 2f. The pattern is shown in Fig. 5a3 (the intensity distribution in this pattern differs slightly from Fig. 2f, since a larger beam waist ($w_0 = 100$ μm instead of 70 μm) was used in the calculation; the pattern sizes are only determined by the phase profile and are independent of the beam waist). As is seen from Figs. 5a1 and 5a2,

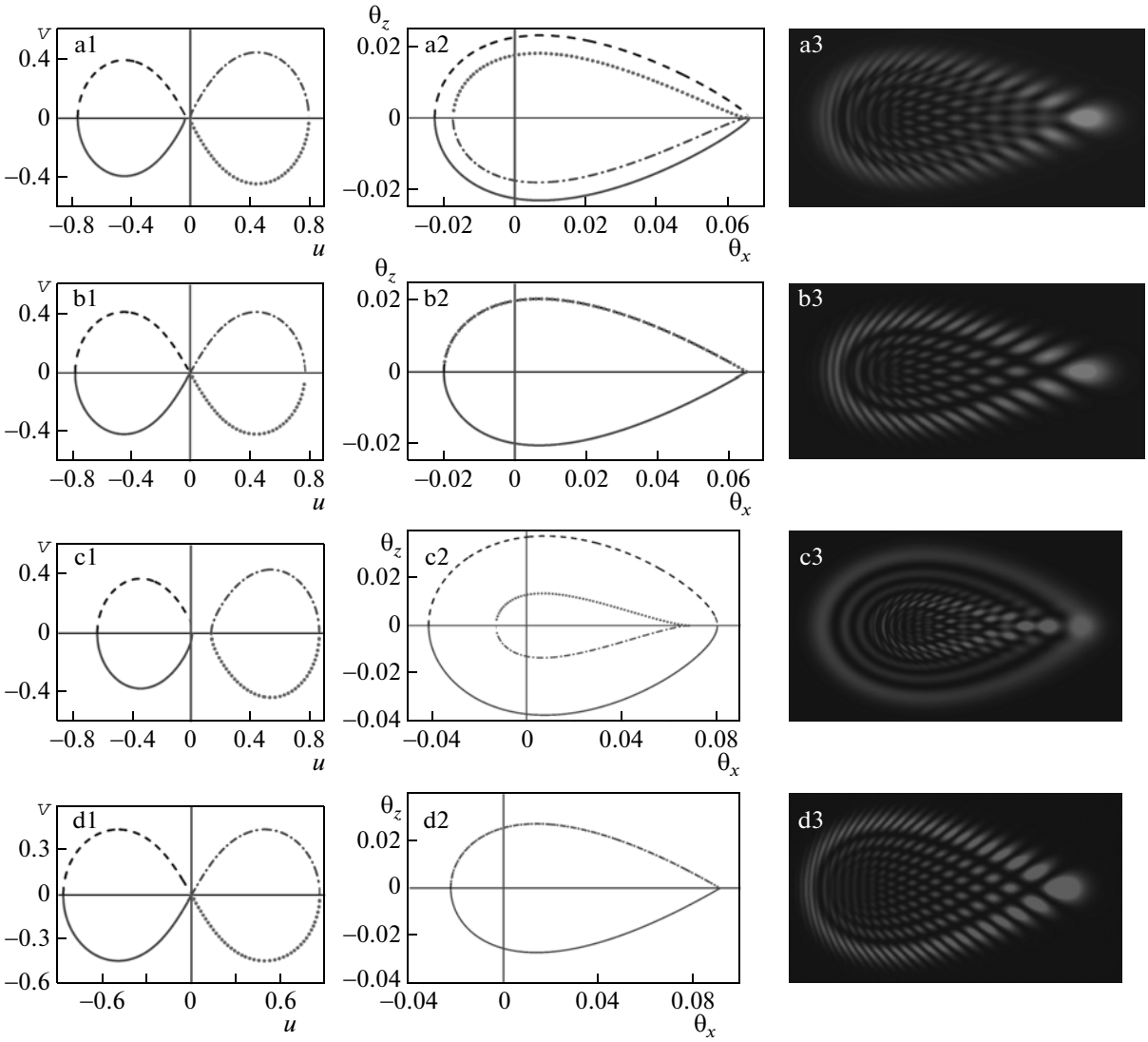

Fig. 5. Calculated (a1–d1) critical points of the mapping $(u, v) \longrightarrow (\theta_x, \theta_z)$, (a2–d2) caustics, and (a3–d3) aberration patterns ($\lambda = 515$ nm, $\Delta n = 0.2$, $L = 100$ μm, $\beta = 30°$, $l_A = l_C = 150$ μm, $w_0 = 100$ μm, $\gamma_A = \sqrt{0.6}$): (a1–a3) $\gamma_C = 0$, $\eta = 0$, phase shift S_{NL} includes terms quadratic in the angle of director rotation; (b1–b3) $\gamma_C = 0$, $\eta = 0$, phase shift S_{NL} does not include terms quadratic in ψ; (c1–c3) $\gamma_C = -\sqrt{0.1}$, $\eta = 0$, terms quadratic in ψ are taken into account; and (d1–d3) $\gamma_C = 0$, $\eta = \sqrt{0.1}$, terms quadratic in ψ are not taken into account. The solid, dashed, dotted, and dot-and-dash sections of the curves in the first and second columns correspond to each other.

the set of critical points and caustics consist of two closed curves. The left and right curves in Fig. 5a1 correspond to the external and internal curves in Fig. 5a2 and the left and right bells in Fig. 4.

The experimentally observed intensity redistribution when the NLC shifts upward (illumination of the lower boundary of the aberration pattern and a decrease in the upper-boundary intensity; see Fig. 2b) does correspond to the negative sign of self-action (self-defocusing) for the external caustic line (Fig. 5a2). The illumination of the top part of the pattern (Fig. 2b, dashed line) corresponds to the visualization of the internal caustic line. The transformation of the aberration pattern when the crystal shifts down is explained similarly. If the crystal shifts to the left, the phase profile is mainly controlled by the right self-focusing bell with a lower divergence (internal caustic line). When the crystal shifts to the right, no visible decrease in the angular spread of the beam is observed.

3.4. Analytical Calculation of the Phase Shift and Caustics

At $\gamma_C = 0$ (screening is only removed at the anode), the rays passing near point O_Σ (i.e., the rays with coordinates close to point $u = v = 0$) undergo the maxi-

mum deflection in the horizontal direction. It is these rays that form the break at the aberration pattern boundary. Let us analytically study this part of the aberration pattern. To this end, we assume for simplicity that $\gamma_G = 0$ (high degree of screening of the applied electric field) and expand phase shifts (17) and (18) near point $u = v = 0$,

$$S_{NL}^{(1)} = 2S_0\gamma_A^2\sin\beta[u - 3u(u^2 + v^2)], \quad (22)$$

$$S_{NL}^{(2)} = -\frac{S_0\cos 2\beta}{\cos\beta}\gamma_A^4 u^2. \quad (23)$$

It is convenient to represent their sum as

$$S_{NL} = S_0\{P[u - 3u(u^2 + v^2)] - Qu^2\}, \quad (24)$$

where

$$P = 2\gamma_A^2\sin\beta, \quad Q = \frac{\cos 2\beta}{\cos\beta}\gamma_A^4.$$

Equation (24), which was obtained by expanding the phase shift into a Taylor series, corresponds to a singularity (catastrophe) of the purse type (or hyperbolic umbilic).

We substitute Eq. (24) into Eqs. (1) and (3) and obtain

$$\theta_x = \theta_{0x}P(1 - 9u^2 - 3v^2 - 36\Delta u), \quad (25)$$

$$\theta_z = -6\theta_{0z}Puv, \quad (26)$$

$$(u + \Delta)^2 - v^2/3 = \Delta^2, \quad (27)$$

where

$$\theta_{0x} = \frac{8\delta n_e L}{\pi^2 l_A\cos\beta}, \quad \theta_{0z} = \theta_{0x}\cos\beta, \quad \Delta = \frac{Q}{18P}.$$

The solution to Eq. (27) is represented by a hyperbola the parametric equations of which have the form

$$u_{L,R} = -\Delta + \gamma_{L,R}\Delta\cosh\tau, \quad v_{L,R} = \sqrt{3}\Delta\sinh\tau. \quad (28)$$

The values $\gamma_L = -1$ and $\gamma_R = +1$ correspond to the left and right branches, respectively (see Figs. 6a, 6c). We substitute Eqs. (28) into Eqs. (25) and (26) and obtain the following parametric equations for the caustics:

$$(\theta_x)_{L,R} = \theta_{0x}P\left[1 + 18\Delta^2\left(1 - \gamma - \sinh^2\tau - 2\gamma\sinh^2\frac{\tau}{2}\right)\right], \quad (29)$$

$$(\theta_z)_{L,R} = 6\sqrt{3}\theta_{0z}P\Delta^2\sinh\tau\left(1 - \gamma - 2\gamma\sinh^2\frac{\tau}{2}\right). \quad (30)$$

Dependences (29) and (30) are graphically illustrated in Figs. 6b and 6d, respectively. It is seen from Fig. 6 that analytical solutions (29) and (30) derived from elementary catastrophe (24) agree well with the exact solutions obtained numerically for phase shift (16) in the vicinity of points $u = 0$, $v = 0$ and $\theta_x = \theta_{0x}$, $\theta_z = 0$.

At low values of τ, the parametric equations for the caustics corresponding to the left and right branches have the form

$$(\theta_x) = \theta_{0x}P(1 + 36\Delta^2 - 9\Delta^2\tau^2), \quad (\theta_z)_L = 12\sqrt{3}\theta_{0z}P\Delta^2\tau, \quad (31)$$

$$(\theta_x)_R = \theta_{0x}P(1 - 27\Delta^2\tau^2), \quad (\theta_z)_R = 3\sqrt{3}\theta_{0z}P\Delta^2\tau^3. \quad (32)$$

As follows from these relationships, the angular distance between the caustics along the x axis is $\delta\theta_x = 36\theta_{0x}P\Delta^2$. This distance for the parameters used in the calculations whose results are shown in Figs. 2a and 5a is 8.5×10^{-4} rad and accounts for less than 1% of the total pattern divergence.

If we neglect the $S_{NL}^{(2)}$ terms in Eq. (16), we should assume $Q = 0$ in Eq. (24) and $\Delta = 0$ in Eqs. (25)–(27). Then, the set of critical points consists of two straight lines,

$$v^{(\pm)} = \pm\sqrt{3}u^{(\pm)}. \quad (33)$$

The parametric equations of the corresponding caustics are as follows:

$$\theta_z^{(\pm)} = \theta_0P(1 - 18\tau^2), \quad \theta_z^{(\pm)} = \mp 6\sqrt{3}\theta_0P\tau^2. \quad (34)$$

Dependences (33) and (34) are shown in Figs. 6e–6h. It is seen in Fig. 6 that the analytical solutions agree well with the corresponding exact solutions, as in the case of $\Delta \neq 0$ considered above.

Parameter Δ specifies the character of the critical set and caustics. As noted above, this parameter vanishes when the quadratic term in expansion (14) is neglected. In this approximation, the nonlinear phase shift is antisymmetric (changes its sign) upon the substitution $u \longrightarrow -u$, which, in turn, reflects the antisymmetry of the x component of the director field (see Fig. 3). As a result, the two caustic curves merge (see Figs. 5b2, 6f, 6h). Point $u = 0$, $v = 0$, $S_{NL}(0, 0) = 0$ in the surface of the nonlinear phase shift becomes umbilic, i.e., a point where all normal sections have the same (in our case, zeroth) curvature.

The antisymmetry of the director field noted above is also violated if $\gamma_C \neq 0$ (light-induced screening removal occurs at both the anode and cathode). Figure 5c shows the set of critical points, caustics, and aberration patterns calculated at $\gamma_C = -\sqrt{0.1}$. It is seen that a possible screening removal at the cathode leads to a significant increase in the difference between the two caustic curves.

In experiment, such a situation is likely to take place in NLCs doped with a methyl red dye [29] and

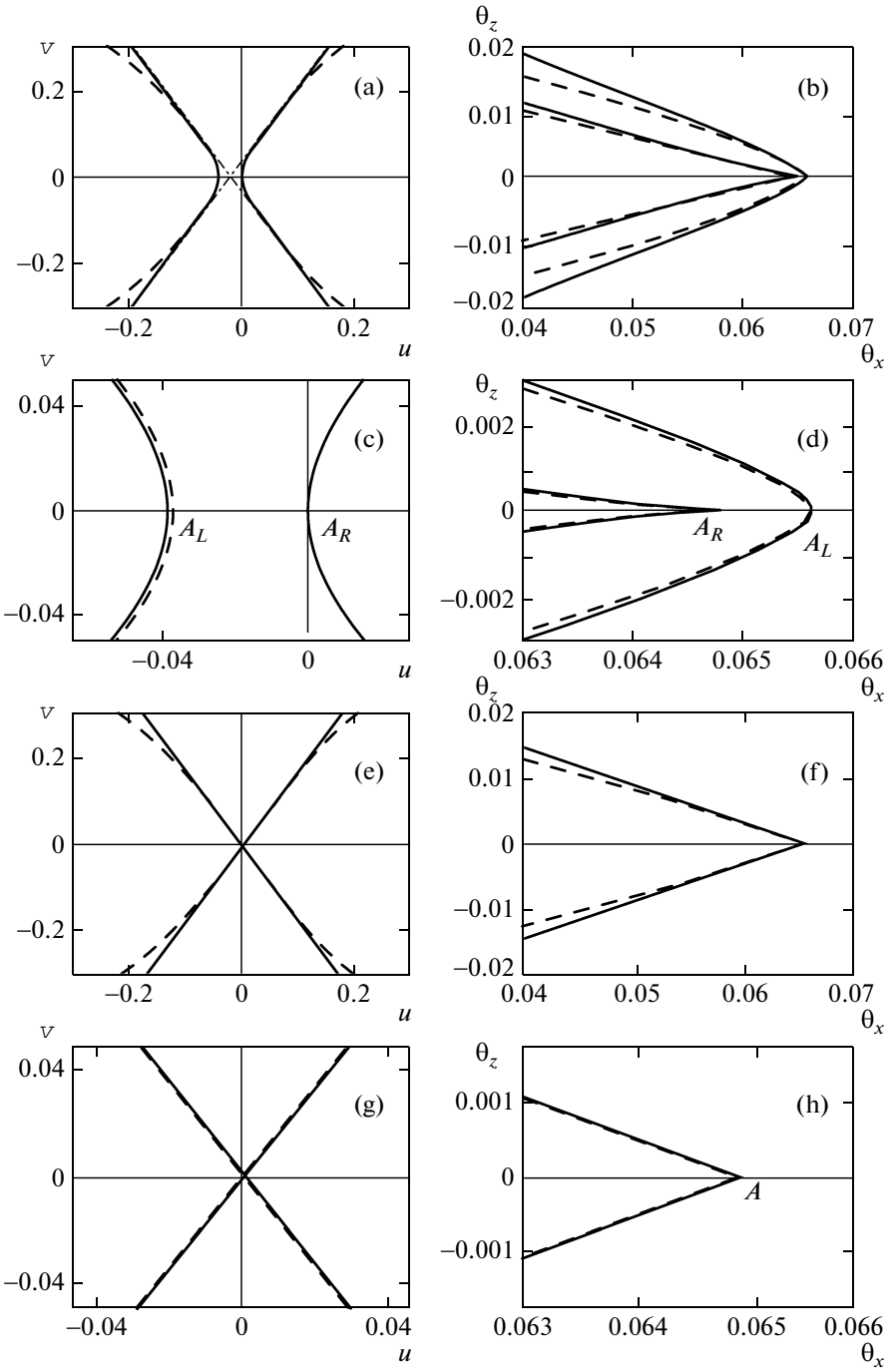

Fig. 6. (a, c, e, g) Critical points of the mapping $(u, v) \longrightarrow (\theta_x, \theta_z)$ near point $(u = 0, v = 0)$. (b, d, f, h) Aberration pattern caustics ($\lambda = 515$ nm, $\Delta n = 0.2$, $L = 100$ μm, $\beta = 30°$, $l_A = 150$ μm, $\gamma_A = \sqrt{0.6}$) calculated for a phase shift (a–d) with and (e–h) without regard for terms quadratic in the angle of director rotation and shown on various scales. (solid lines) Calculations by (a, c) Eq. (28), (e, g) Eq. (33), (b, d) Eqs. (29) and (30), and (f, d) Eqs. (31) and (32). (dashed lines) Numerical solutions to Eq. (3) and their images (1) and (dot-and-dash straight lines in Fig. 6a) asymptotes of hyperbola (33).

dendrimers [39]. The corresponding aberration patterns are shown in Figs. 1c and 1d. Physically, the difference in the behavior of pure and dye-doped samples can be caused by the deposition of dyes on the liquid-crystal cell walls [40, 41].

A homogeneous field penetrating into the NLC volume ($\gamma_G \neq 0$) increases the aberration pattern divergence (as is seen from a comparison of Figs. 5d and 5a). However, it does not break the antisymmetry of the director field and does not cause the separation

of caustics in the absence of a quadratic term in the phase shift.

4. CONCLUSIONS

We studied the main properties of the self-action of a light beam in an NLC placed in a dc electric field.

Based on the proposed mechanism of the surface photorefractive effect (which consists in the reorientation of a director in a dc electric field and is caused by the light-induced removal of screening), we developed a theory for the self-action of a light beam in an NLC. The effect of light was simulated by a field of point charges.

The self-action of light in an NLC was shown to result in singularities of the purse type (or hyperbolic umbilic catastrophe). The aberration pattern was calculated, and the caustics of the light beam were analyzed. The calculation results well describe the experimental data.

Note that, in nonlinear optics, the self-action of light beams usually leads to a ring pattern, which corresponds to the simplest singularity of the fold type. The authors of [42] reported the appearance a cusp singularity during the thermal self-action of a light beam that was not axially symmetric. A purse-type singularity (hyperbolic umbilic catastrophe) was observed on orientational nonlinearities in an NLC during the interaction of two light beams [43] and in the particular case of this geometry [44], where a light beam reflected from an NLC boundary and repeatedly passed through the liquid-crystal layer (here, the weak reflected beam did not affect the director orientation). The appearance of this singularity for a single pass of an axially symmetric light beam through a nonlinear medium is likely to be detected for the first time in the considered case of the interaction of light with an NLC in a dc electric field.

When addressing examples from linear optics, we note that the asymmetric pattern detected in the far diffraction zone in this work resembles the intensity distribution in the image of a point source generated by a lens with comatic aberration (similarly to the fact that a usual ring pattern is analogous to the spherical aberration of a lens) [45]. Note also that purse-type singularities were detected during light scattering by drops [46, 47].

The analytical expressions obtained in this work for a nonlinear phase shift can be used to describe the light intensities in the caustics of an aberration pattern.

ACKNOWLEDGMENTS

The authors are grateful to V.N. Ochkin for continuous interest in our work and useful discussions.

This work was supported by the Russian Foundation for Basic Research (project nos. 08-02-01382-a and 09-02-12216-ofi_m), grant of the President of the Russian Federation (project no. MK-699.2009.2), the Program of Support for Young Scientists of the Presidium of the Russian Academy of Sciences (I.A.B. and M.P.S.), the Federal Program "Scientific and Scientific–Pedagogical Personnel of Innovation Russia" (State contract no. 02.740.11.0447), and the Russian Science Support Foundation (M.P.S.).

REFERENCES

1. P. de Gennes, *The Physics of Liquid Crystals* (Clarendon, Oxford, 1974; Mir, Moscow, 1977).
2. L. M. Blinov, *Electro- and Magneto-Optics of Liquid Crystals* (Nauka, Moscow, 1978) [in Russian].
3. B. Ya. Zel'dovich, N. F. Pilipetskii, A. V. Sukhov, and N. V. Tabiryan, Pis'ma Zh. Éksp. Teor. Fiz. **31** (5), 287 (1980) [JETP Lett. **31** (5), 263 (1980)].
4. I. Janossy, L. Csillag, and A. D. Lloyd, Phys. Rev. A: At., Mol., Opt. Phys. **44**, 8410 (1991).
5. I. A. Budagovsky, A. S. Zolot'ko, V. N. Ochkin, M. P. Smayev, A. Yu. Bobrovsky, V. P. Shibaev, and M. I. Barnik, Zh. Éksp. Teor. Fiz. **133** (1), 204 (2008) [JETP **106** (1), 172 (2008)].
6. A. S. Zolot'ko, V. F. Kitaeva, N. Kroo, N. N. Sobolev, and L. Chillag, Pis'ma Zh. Éksp. Teor. Fiz. **32** (2), 170 (1980) [JETP Lett. **32** (2), 158 (1980)].
7. A. S. Zolot'ko, V. F. Kitaeva, N. N. Sobolev, and A. P. Sukhorukov, Zh. Éksp. Teor. Fiz. **81** (3), 933 (1981) [Sov. Phys. JETP **54** (3), 496 (1981)].
8. S. D. Durbin, S. M. Arakelian, and Y. R. Shen, Opt. Lett. **6**, 411 (1981).
9. A. S. Zolot'ko, V. F. Kitaeva, N. Kroo, N. N. Sobolev, A. P. Sukhorukov, and L. Chillag, Zh. Éksp. Teor. Fiz. **83** (4), 1368 (1982) [Sov. Phys. JETP **83** (4), 786 (1982)].
10. I. C. Khoo, S. L. Zhuang, and S. Shepard, Appl. Phys. Lett. **39**, 937 (1981).
11. E. Santamato and Y. R. Shen, Opt. Lett. **9**, 564 (1984).
12. C. Conti, M. Peccianti, and G. Assanto, Phys. Rev. Lett. **92**, 113902 (2004).
13. J. F. Henninot, J. F. Blach, and M. Warenghem, J. Opt. A: Pure Appl. Opt. **10**, 085104 (2008).
14. V. F. Kitaeva, A. S. Zolot'ko, and M. I. Barnik, Mol. Mater. **12**, 271 (2000).
15. I. Janossy and T. Kosa, Opt. Lett. **17**, 1183 (1992).
16. S. A. Akhmanov, Yu. A. Gorokhov, D. P. Krindach, A. P. Sukhorukov, and R. V. Khokhlov, Zh. Éksp. Teor. Fiz. **57** (1), 16 (1969) [Sov. Phys. JETP **30** (1), 9 (1970)].
17. F. W. Dabby, T. K. Gustafson, J. R. Whinnery, and Y. Kohanzadeh, Appl. Phys. Lett. **16**, 362 (1970).
18. A. S. Zolot'ko, V. F. Kitaeva, V. A. Kuyumchyan, N. N. Sobolev, and N. N. Sukhorukov, Pis'ma Zh. Éksp. Teor. Fiz. **36** (3), 66 (1982) [JETP Lett. **36** (3), 80 (1982)].
19. G. Cipparrone, D. Duca, C. Umeton, and N. V. Tabiryan, Phys. Rev. Lett. **71**, 3955 (1993).
20. A. S. Zolot'ko, V. F. Kitaeva, N. Kroo, N. N. Sobolev, A. P. Sukhorukov, V. A. Troshkin, and L. Chillag, Zh. Éksp. Teor. Fiz. **87** (3), 859 (1984) [Sov. Phys. JETP **60** (3), 488 (1984)].

21. A. S. Zolot'ko and V. F. Kitaeva, Zh. Éksp. Teor. Fiz. **91** (1), 131 (1986) [Sov. Phys. JETP **64** (1), 76 (1986)].
22. L. Csillag, N. Eber, I. Janossy, N. Kroo, V. F. Kitaeva, and N. N. Sobolev, Mol. Cryst. Liq. Cryst. **89**, 287 (1982).
23. M. I. Barnik, S. A. Kharchenko, V. F. Kitaeva, and A. S. Zolot'ko, Mol. Cryst. Liq. Cryst. **375**, 363 (2002).
24. S.-H. Chen and J. J. Wu, Appl. Phys. Lett. **52**, 1998 (1988).
25. J. J. Wu, G.-S. Ong, and S.-H. Chen, Appl. Phys. Lett. **53**, 1999 (1988).
26. J. J. Wu and S.-H. Chen, J. Appl. Phys. **66**, 1065 (1989).
27. A. S. Zolot'ko, M. P. Smaev, V. F. Kitaeva, and M. I. Barnik, Kvantovaya Élektron. (Moscow) **34**, 1151 (2004) [Quantum Electron. **34**, 1151 (2004)].
28. I. A. Budagovsky, A. S. Zolot'ko, V. F. Kitaeva, V. N. Ochkin, M. P. Smayev, and M. I. Barnik, Kratk. Soobshch. Fiz., No. 3, 24 (2006) [Bulletin of the Lebedev Physics Institute, No. 3, 18 (2006)].
29. A. S. Zolot'ko, I. A. Budagovsky, V. F. Kitaeva, V. N. Ochkin, A. V. Shakun, M. P. Smayev, and M. I. Barnik Mol. Cryst. Liq. Cryst. **454**, 407 (2006).
30. L. Csillag, I. Janossy, V. F. Kitaeva, N. Kroo, N. N. Sobolev, and A. S. Zolotko, Mol. Cryst. Liq. Cryst. **78**, 173 (1981).
31. V. I. Arnol'd, Usp. Fiz. Nauk **141** (4), 569 (1983) [Sov. Phys.–Usp. **26** (12), 1025 (1983)].
32. Yu. A. Kravtsov and Yu. I. Orlov, Usp. Fiz. Nauk **141** (4), 591 (1983) [Sov. Phys.–Usp. **26** (12), 1038 (1983)].
33. R. Gilmore, *Catastrophe Theory for Scientists and Engineers* (Wiley, New York, 1981; Mir, Moscow, 1984), Vol. 1.
34. T. Poston and I. Stewart, *Catastrophe Theory and Its Applications* (Pitman, London, 1978; Mir, Moscow, 1980).
35. M. V. Berry and C. Upstill, in *Progress in Optics*, Ed. by E. Wolf (North-Holland, Amsterdam, 1980), Vol. XVIII, p. 257.
36. M. V. Berry, Adv. Phys. **25**, 1 (1976).
37. W. Stewart, *The Static and Dynamic Continuum Theory of Liquid Crystals* (Taylor and Francis, London, 2004), p. 79.
38. L. D. Landau and E. M. Lifshitz, *Course of Theoretical Physics*, Vol. 7: *Theory of Elasticity* (Nauka, Moscow, 1987; Butterworth–Heinemann, Oxford, 1995).
39. I. A. Budagovsky, V. N. Ochkin, M. P. Smayev, A. S. Zolot'ko, A. Yu. Bobrovsky, N. I. Boiko, A. I. Lysachkov, V. P. Shibaev, and M. I. Barnik, Liq. Cryst. **36**, 101 (2009).
40. E. Ouskova, Yu. Reznikov, S. V. Shiyanovskii, L. Su, J. L. West, O. V. Kuksenok, O. Francescangeli, and F. Simoni, Phys. Rev. E: Stat., Nonlinear, Soft Matter Phys. **64**, 051709 (2001).
41. M. I. Barnik, V. F. Kitaeva, and A. S. Zolot'ko, Mol. Cryst. Liq. Cryst. **391**, 111 (2003).
42. A. M. Deykoon, M. S. Soskin, and G. A. Swartzlander, Jr., Opt. Lett. **24**, 1224 (1999).
43. N. V. Tabiryan, B. Ya. Zel'dovich, M. Kreuzer, and T. Vogeler, J. Opt. Soc. Am. B **13**, 1426 (1996).
44. I. A. Budagovsky, A. S. Zolot'ko, V. F. Kitaeva, and M. P. Smayev, Mol. Cryst. Liq. Cryst. **453**, 71 (2006).
45. M. Born and E. Wolf, *Principles of Optics* (Pergamon, London, 1959; Nauka, Moscow, 1973).
46. J. F. Nye, Nature (London) **312**, 531 (1984).
47. G. Kaduchak and P. L. Marston, Appl. Opt. **33**, 4697 (1994).

Translated by K. Shakhlevich